RSNA Press Release

Photon-counting CT Outperforms Conventional CT in Lung Cancer Management

Released: February 3, 2026

Songwei Yue, M.D.

OAK BROOK, Ill. – In a prospective imaging study of 200 adults with lung cancer, photon-counting CT reduced radiation exposure, had fewer adverse reactions and provided higher image quality and better detection of malignant features compared with conventional CT. Results of the study were published today in *Radiology*, a journal of the Radiological Society of North America (RSNA).

Lung cancer is the leading cause of cancer mortality, accounting for 18.7% of deaths globally. To characterize lung tumors and support personalized therapeutic strategies, doctors use CT imaging. Photon-counting CT is an advanced medical imaging technology that directly counts and measures the energy of individual X-ray photons, unlike conventional CT, which averages them. The result is sharper, higher-resolution images and better tissue differentiation.

“Effective follow-up of cancer patients enhances early detection and survival, with regular imaging identifying recurrence in 60 to 100% of cases,” said Songwei Yue, M.D., chief physician, professor and deputy director of radiology in the Department of Radiology at The First Affiliated Hospital of Zhengzhou University in Henan, China.

However, the cumulative radiation and exposure to contrast media involved in conventional CT imaging pose challenges for lung cancer patients, including the possibility of contrast-induced acute kidney injury. According to Dr. Yue, implementing radiation-reduction strategies for CT is challenging, because it can lead to diagnostic errors.

In the study, researchers compared the benefits of contrast-enhanced chest CT using ultra-high-resolution photon-counting CT versus conventional CT across different populations and body mass indices (BMIs) between June and December 2024. Adverse reactions were documented within one hour after contrast agent injection, and baseline renal function parameters were assessed within 48 hours post-injection.

A radiologist experienced in chest imaging performed measurements using a 5-point Likert scale to analyze lesion image quality, malignant radiological features, diagnostic confidence, BMI subgroup and tumor size. Two experienced chest radiologists independently evaluated the noise, anatomical structures, lesion sharpness, structures within enhanced lesions and overall image quality.

Patients were analyzed in subgroups based on lesion size (≤ 3cm or >3cm) and BMI. Objective image quality and subjective scores were compared among BMI subgroups.

The researchers formed two study groups of 100 individuals, matched on 13 parameters, including weight, age, histological type, T-staging and kidney function. The first group of 100 (61 males, mean age 61) underwent low-dose photon-counting CT, and in the second group (65 males, mean age 61) underwent conventional CT.

Compared to conventional CT, photon-counting CT reduced radiation and iodine exposure by 66.34% and 26.57%,

respectively. Individuals who underwent low-dose ultra-high resolution photon-counting CT also had fewer adverse reactions, including contrast-induced acute kidney injury, compared to conventional CT. At a 0.4 mm section thickness, photon-counting CT improved overall image quality, detection of enhancement-related malignant features, and diagnostic confidence, making it suitable for various BMI and small lesions at the T1 stage.

“Compared with conventional CT, low-dose, ultra-high-resolution photon-counting CT improves the detection of enhancement-related malignant features across varying BMI and tumor sizes,” Dr. Yue said. “It enhanced diagnostic confidence while reducing radiation exposure and contrast media use.”

The researchers said future studies should include longitudinal follow-up scans on the same participants to compare the performance of photon-counting CT in long-term lung cancer monitoring and treatment assessment.

“We believe photon-counting CT might replace conventional CT in the near future due to its improved imaging quality and the diagnostic confidence it offers,” Dr. Yue said.

“Photon-counting CT versus Energy-integrating Detector CT Performance for Various BMI and Tumor Sizes in Lung Cancer.” Collaborating with Dr. Yue were Yuhan Zhou, M.D., Xiaoxu Guo, M.D., Limin Lei, M.D., Haojie Zhang, M.D., Zhihao Wang, M.D., Yifan Guo, M.D., Yajie Wang, M.D., Lina Tao, M.D., and Hao Sun, M.D.

Radiology is edited by Suhny Abbara, M.D., FACR, MSCCT, Mayo Clinic, Jacksonville, Florida, and owned and published by the Radiological Society of North America, Inc. (https://pubs.rsna.org/journal/radiology)

RSNA is an association of radiologists, radiation oncologists, medical physicists and related scientists promoting excellence in patient care and health care delivery through education, research and technologic innovation. The Society is based in Oak Brook, Illinois. (RSNA.org)

For patient-friendly information on chest CT, visit *RadiologyInfo.org*.

Images (JPG, TIF):

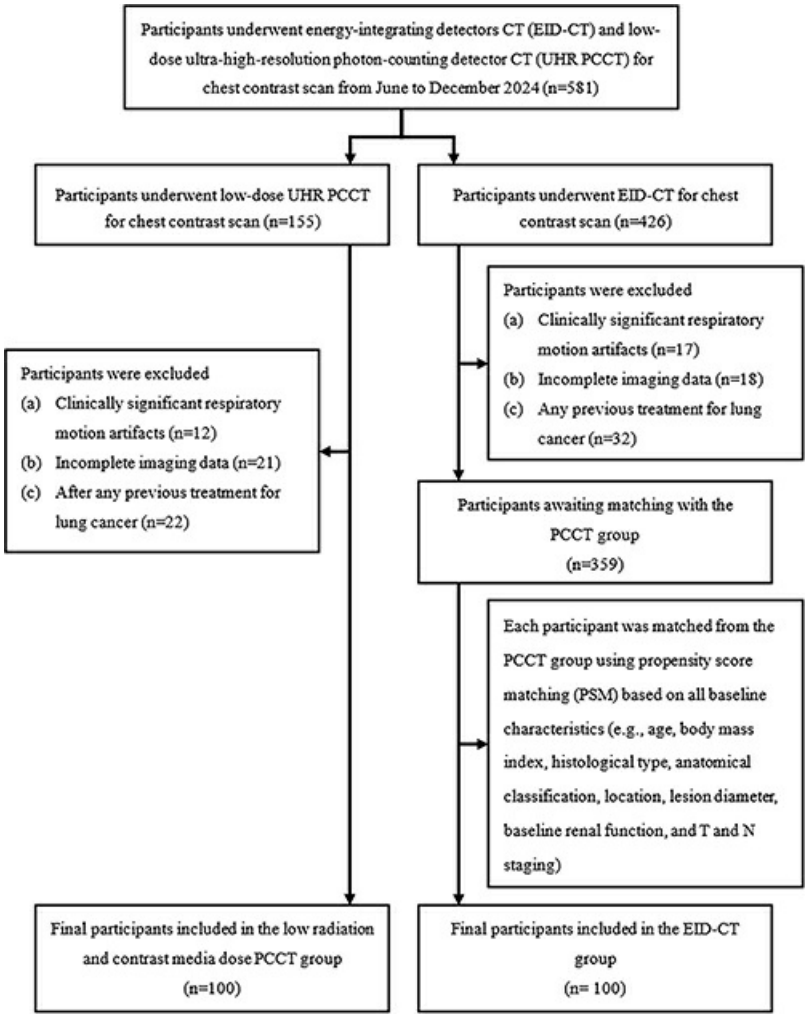

Figure 1. Flowchart of the study design. EID = energy-integrating detector, PCCT = photon-counting CT, UHR = ultrahigh resolution.

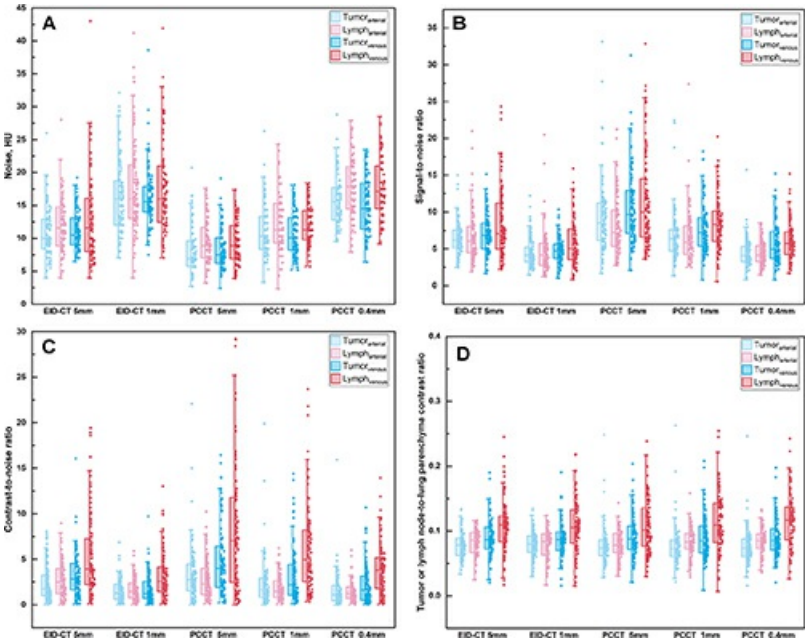

Figure 2. Objective image quality comparison. Half-box plots show the **(A)** noise, **(B)** signal-to-noise ratio, **(C)** contrast-to-noise ratio, and **(D)** tumor or lymph node–to-lung parenchyma contrast ratio of the tumor and lymph

node in the arterial and venous phases based on photon-counting CT (PCCT) and energy-integrating detector (EID) CT after propensity score matching. The midline represents the median, box boundaries indicate the IQR, and the whisker boundaries extend to the minimum and maximum values of the data. Dots show the exact location of data.

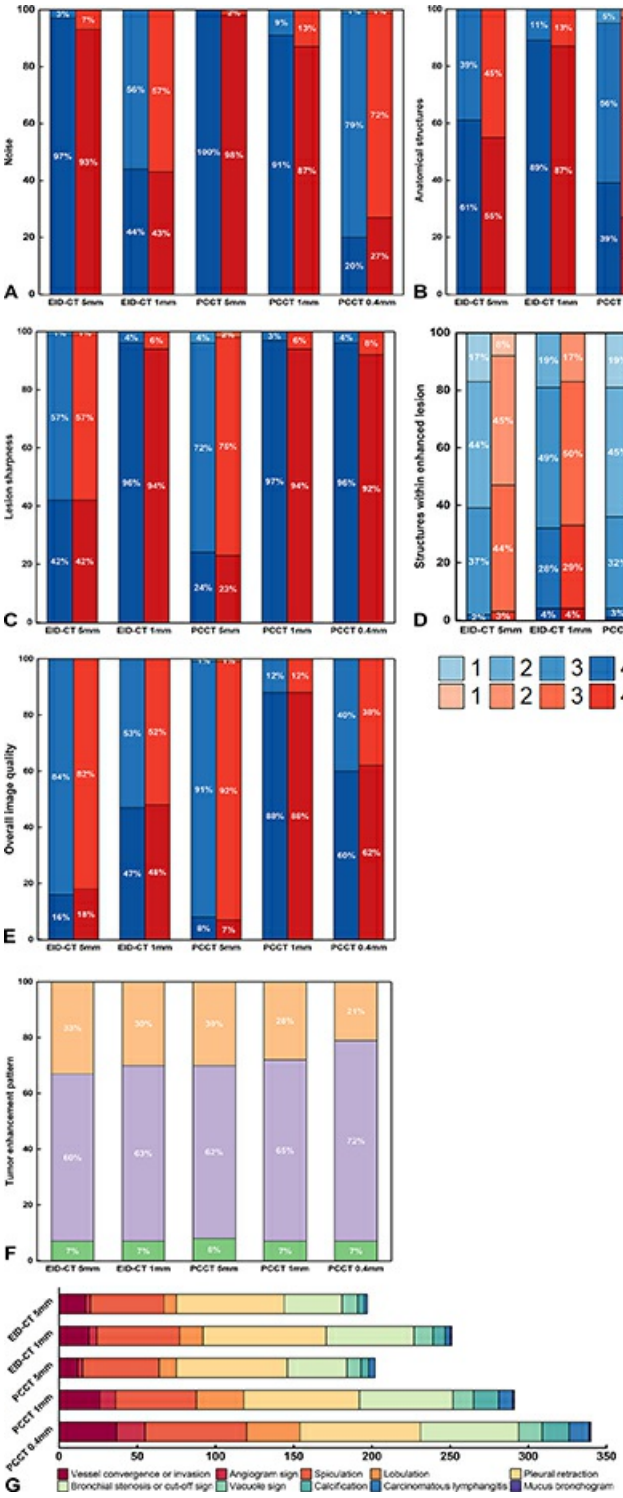

Figure 3. (A–E) Comparison of subjective image quality after propensity score matching. Stacked bar graphs with ratings show the **(A)** noise, **(B)** anatomic structures, **(C)** lesion sharpness, **(D)** structures within enhanced lesion, and **(E)** overall image quality scores of energy-integrating detector (EID) CT and photon-counting CT (PCCT) images by two readers (five-point scale: high quality and diagnostic value, ≥3; poor and insufficient for diagnosis, >3). The κ values between the two readers were 0.89 for noise, 0.80 for anatomic structures, 0.88 for lesion sharpness, 0.85 for structures within enhanced lesion, and 0.92 for overall image quality. **(F)** Stacked bar graph shows comparison of tumor enhancement pattern. **(G)** Stacked bar plot shows detection numbers of malignancy-related imaging features.

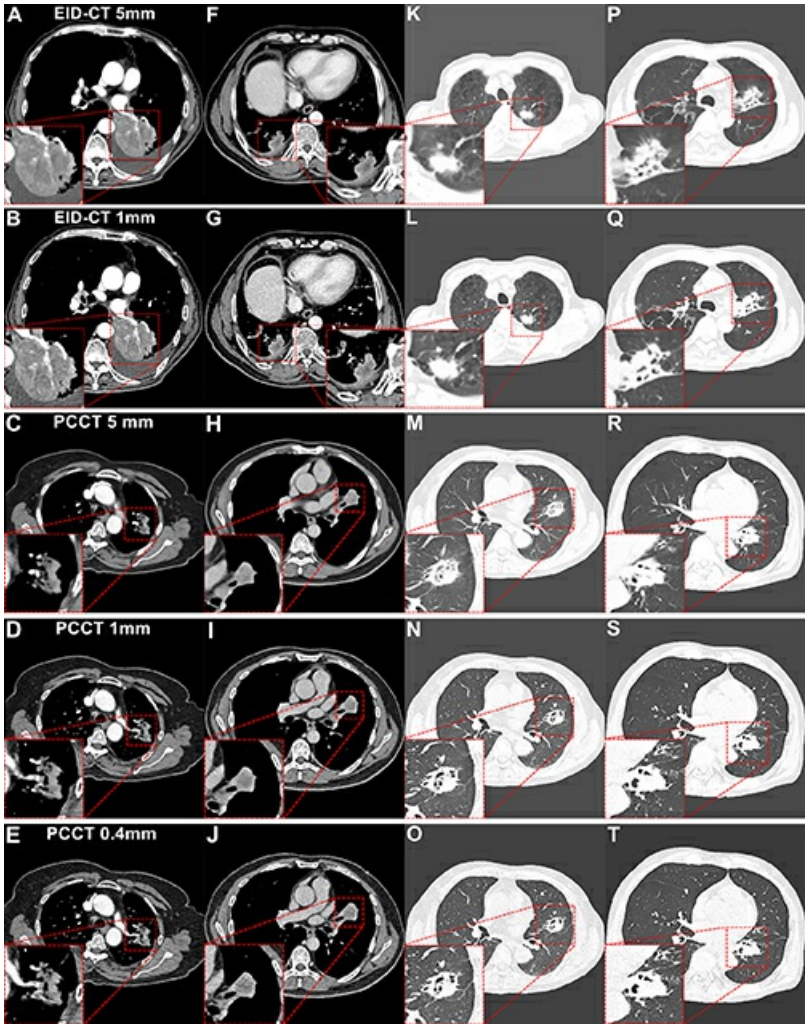

Figure 4. Contrast-enhanced chest CT images of lung cancer from energy-integrating detector (EID) CT and photon-counting CT (PCCT). The red outlined areas highlight the magnified images of lesions. **(A–E)** Vessel convergence or invasion sign in the axial images of the arterial phase. **(A, B)** EID CT images in a 74-year-old man with a body mass index (BMI) of 18.6, calculated as weight in kilograms divided by height in meters squared, diagnosed with adenocarcinoma. **(C–E)** PCCT images in a 72-year-old woman (BMI, 20.0) diagnosed with adenocarcinoma. The vessels' delineation and continuity are more distinct in PCCT 0.4-mm images. **(F–J)** The boundary of the necrotic area within the tumor in the axial images of the venous phase. **(F, G)** EID CT images in a 62-year-old man (BMI, 23.8) diagnosed with squamous cell carcinoma. **(H–J)** PCCT images in a 60-year-old man (BMI, 23.6) diagnosed with squamous cell carcinoma. The improved spatial resolution and iodine signal of PCCT enhance the delineation of the necrotic area boundary within the tumor, particularly in the 0.4-mm images. (K–O) Lobulation, spiculation, and pleural retraction in the axial images with lung windows. **(K, L)** EID CT images in an 82-year-old man (BMI, 20.8) diagnosed with adenocarcinoma. **(M–O)** PCCT images in a 72-year-old man (BMI, 23.5) diagnosed with adenocarcinoma. Compared with EID CT and other section thicknesses, PCCT at 0.4 mm demonstrates better diagnostic confidence for subtle spiculations, shallow lobulations, and pleural traction lines. **(P–T)** Bronchial stenosis or cutoff sign in the axial images with lung windows. **(P, Q)** EID CT images in a 70-year-old man (BMI, 20.5) diagnosed with squamous cell carcinoma. **(R–T)** PCCT images in a 58-year-old man (BMI, 21.8) diagnosed with squamous cell carcinoma. PCCT at 0.4 mm improves the visualization of stenosis, truncation, and their boundary morphology relative to EID CT.

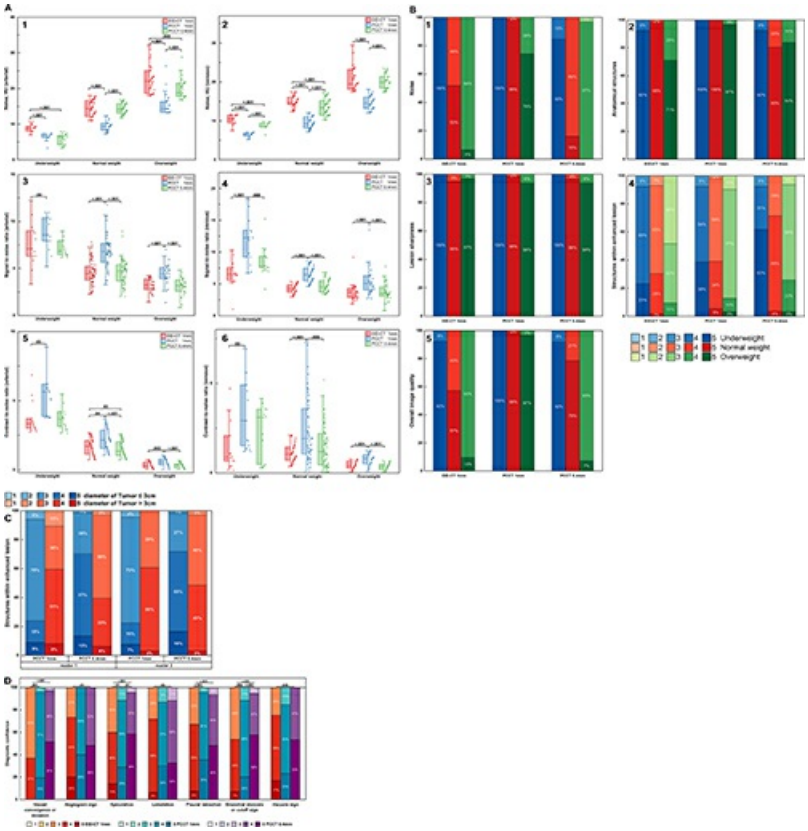

Figure 5. (A) Comparison of objective image quality in body mass index (BMI) subgroups. Half-box plots show the noise, signal-to-noise ratio (SNR), and contrast-to-noise ratio (CNR) of the tumor in the arterial phase and venous phase between photon-counting CT (PCCT) and energy-integrating detector (EID) CT after propensity score matching. The midline represents the median, box boundaries indicate the IQR, and the whisker boundaries extend to the minimum and maximum values of the data. Dots show the exact location of each data. **(B)** Comparison of subjective image quality in BMI subgroups. Stacked bar graphs with ratings show the noise, anatomic structures, lesion sharpness, structures within enhanced lesion, and overall image quality scores of EID CT and PCCT images. **(C)** Stacked bar graphs show subgroup comparison of subjective score of the structures within enhanced lesion based on lesion size. **(D)** Stacked bar graphs show distribution of five-point Likert scale categories for diagnostic confidence in lung cancer radiologic signs (vessel convergence or invasion, angiogram sign, spiculation, lobulation, pleural retraction, bronchial stenosis or cutoff sign, and vacuole sign). The patients were stratified by BMI, calculated as weight in kilograms divided by height in meters squared, as follows: underweight (<18.5), normal weight (18.5-24.9), and overweight (≥25).

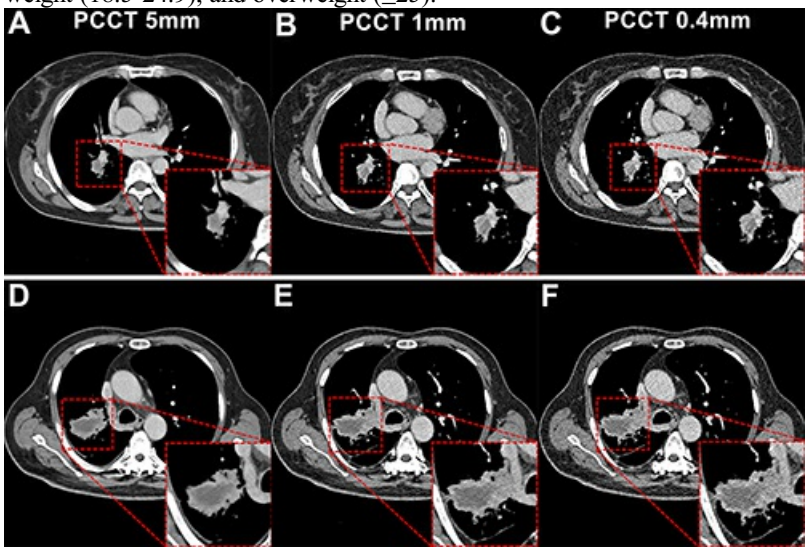

Figure 6. Subgroup analysis based on lesion size on photon-counting CT (PCCT) images. The red outlined areas highlight the magnified images of lesions. **(A–C)** PCCT images in a 62-year-old woman with a body mass index

(BMI) of 23.6, calculated as weight in kilograms divided by height in meters squared, who was diagnosed with adenocarcinoma. A lesion with a long diameter of 25 mm was identified in the right lower lobe on axial images acquired during the venous phase. For lesions less than or equal to 30 mm, decreasing section thickness improved boundary sharpness and contrast between the necrotic area and enhanced tissue, with optimal visualization at 0.4 mm. **(D–F)** PCCT images in a 66-year-old man with a BMI of 24.2 who was diagnosed with adenocarcinoma, revealing a lesion with a long diameter of 52 mm in the right lower lobe. For lesions greater than 30 mm, a section thickness of 1 mm demonstrated better contrast and clarity at the boundary of the necrotic area compared with 0.4 mm. This observation supported the selection of an appropriate section thickness for accurate quantification of necrotic regions within the lesion.

Resources:

Abstract link